Central European Journal of Energetic Materials, **2015**, *12*(1), 63-76
ISSN 2353-1843

Estimation of the Increase in Projectile Velocity in the Intermediate Ballistics Period

Radosław TRĘBIŃSKI, Marta CZYŻEWSKA

Department of Mechatronics and Aviation, Military University of Technology, Gen. S. Kaliskiego 2, 00-908 Warsaw, Poland
E-mails: rkt@wat.edu.pl, marta.czyzewska@wat.edu.pl

Abstract: The idea of the application of internal ballistics models together with external ballistics models in fire control systems encounters a problem in relating the calculated muzzle velocity value to the initial velocity value used in external ballistics calculations. The difference between these two values is caused by the action on the projectile of the propellant gases exiting from the muzzle. In this paper an attempt has been made to estimate the increase in projectile velocity outside the muzzle by the use of CFD modelling. The commercial ANSYS FLUENT code has been used together with our own 1D model for the internal ballistics period. Calculations have been performed for various launching systems, from small arms to a 155 mm calibre gun. Conclusions have been drawn concerning the magnitude of the increase in projectile velocity outside the muzzle. The main conclusion is that the velocity increase is generally less than 1% and in most cases can be neglected.

Keywords: intermediate ballistics, internal ballistics, projectile velocity

List of symbols:

α	− covolume of propellant gases	l_C	− symbol explained in Figure 2
$\Gamma(\psi)$	− dependence of burning rate on relative volume of burnt propellant	l_F	− as above
		l_{FP}	− length of the forward part of the projectile
δ	− density of solid propellant	l_p	− length of the projectile
Δu	− velocity increase	m_p	− mass of the projectile
ε	− specific internal energy	n_x, n_r	− components of normal vector
		p	− pressure

φ – coefficient taking into account frictional resistance and rotational motion of the projectile
ρ – density
ω – loading density of propellant
ψ – relative volume of burnt propellant
c_{02} – initial sound velocity in the air
f – power of propellant
$f_s(p)$ – dependence of burning rate on pressure
$f_{SP}(x)$ – function describing shape of the projectile in a reference frame positioned at its nose
k_1 – polytropic exponent of propellant gases
k_2 – polytropic exponent of the air
p_f – starting value of pressure
p_z – ignition pressure
p_{02} – initial value of air pressure
r – radial coordinate
r_A – symbol explained in Figure 2
r_B – as above
r_D – as above
t – time
t_{k2} – final moment of step two
$x_L(t)$ – position of the tail of the projectile
$x_P(t)$ – position of the nose of the projectile
x_{L0} – initial position of the bottom of the projectile
u_m – the maximum velocity
l_B – position of the burning chamber bottom
u_0 – initial velocity

1 Introduction

The interval of a gunshot, starting at the moment when a projectile leaves the muzzle of a gun, and ending at the moment when the projectile leaves the area perturbed by the propellant gases outflow, is called the intermediate ballistics period. It separates the period of the internal ballistics and the period of the external ballistics. It has been extensively investigated, mainly from the point of view of the possibilities for reducing muzzle blast and flash effects. An extensive review of the results of this investigation was made in monograph [1]. However, there is no information there about the magnitude of the velocity increase in the period of intermediate ballistics. In a classical internal ballistics handbook [2] this increase was assessed to be of the order of 1-2% of the muzzle velocity. However, in more recent monographs devoted to ballistics there is a lack of such information (see *e.g.* [3, 4]).

There are a number of methods for modelling the internal ballistics period, which make it possible to predict the value of the muzzle velocity u_m. There also

exist a number of methods for modelling the external ballistics period. These models use the so-called initial velocity u_0, which is not the same as the muzzle velocity. The difference between these two velocities is explained in Figure 1. It is caused by the action on the projectile of the propellant gases exiting the muzzle. The pressure of the propellant gases does not drop instantaneously to the ambient pressure. Therefore, it additionally accelerates the projectile up to the moment when it drops below the pressure acting on the forward part of the projectile. From this moment the velocity starts to decrease due to aerodynamic drag. The maximum velocity is higher than the muzzle velocity and in this paper we try find an answer to the question: by how much? The initial velocity u_0 is an extrapolation of the decaying part of the $u_p(x)$ curve to the position of the muzzle. For this reason it is higher than the muzzle velocity. But if we know the maximum velocity and the distance from the muzzle at which it is attained, we can use this value instead of the initial velocity u_0. Without information about the changes in the projectile velocity in the intermediate period, it is impossible to find a relation between u_m and u_0.

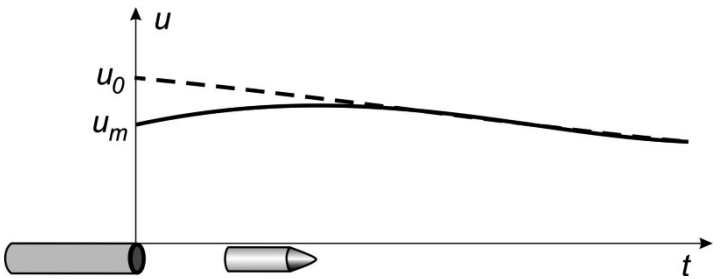

Figure 1. Diagram explaining the difference between the muzzle velocity u_m and the initial velocity u_0.

Simulations of the external ballistics performed in report [5] proved that the relative differences in the calculated ranges are of the same order as the differences between u_m and u_0. Because the accepted tolerance of the calculated range is 0.2% [6], a 1% percent difference between u_m and u_0 may be meaningful. The results of experimental investigations by Doppler radar velocimetry and optical methods presented in [7] suggest that the increase in the velocity in the intermediate ballistics period Δu is of the order given in [2] – up to 2%. However, variations in the measured velocity values were of the same magnitude – [5]. Therefore, we can treat this result as only an upper estimate of Δu. In order to find a more precise estimate we tried to use computational fluid dynamics methods (CFD).

The gas dynamics processes taking place during the intermediate ballistics period have been modelled in a number of studies [8-14]. In all of these the flow around the muzzle was treated as an axi-symmetrical flow of an inviscid perfect gas. The focus was on characterizing the flow field produced by the outflow from the muzzle. No attention was paid to changes in the projectile velocity.

In this paper we present an analysis of the results of CFD modelling of the intermediate ballistics period. The results are analyzed with the aim of determining the magnitude of the velocity increase. The calculations were performed for various launching systems, from small arms to a 155 mm caliber gun. General statements are made concerning the expected values of the magnitude of the velocity increase in the intermediate ballistics period.

2 Description of the model

In the theoretical model presented we consider processes taking place in the internal ballistics period and in the intermediate ballistics period. Modelling of both periods is necessary because the outflow of the air pushed from the barrel by the projectile perturbs the area near the muzzle before the intermediate period starts (this outflow is referred to as the *precursor* – [1]). In the modelling, we assume the following procedure.

2.1 Step 1 – internal ballistics

In the first step, we use a 1D model for modelling the internal ballistics period without taking into account wave processes in the air in front of the projectile. Only an approximation of the pressure of the air acting on the front side of the projectile is used. This pressure is at least two orders of magnitude lower than the pressure of propellant gases driving the projectile. Hence it has no significant influence on the value of the velocity of the projectile, which justifies such an approach. As a result of the modelling, we obtain a history of the motion of the projectile $u_p(t)$ and spatial distributions of pressure $p(x)$, density $\rho(x)$ and velocity $u(x)$ of the propellant gases at the moment of the beginning of an outflow of the gases.

There is a problem in choosing which moment in time is the final moment of the internal ballistics period. Leakage of the propellant gases begins when the driving band of the projectile leaves the muzzle. However, we have made a simplifying assumption that the outflow of gases begins at the moment when the flat tail of the projectile leaves the muzzle. This assumption causes the presented model to overestimate the velocity increase. However, one of the objectives of the modelling was to assess an upper limit of the velocity increase.

The mathematical model for the first step is given by the following initial-boundary problem (the reference frame is the same as in Figure 3):

$$\begin{gathered}\rho_{,t}+\left(\rho u_x\right)_{,x}+\rho u_x\left(\ln S\right)_{,x}=0\\ u_{x,t}+u_x u_{x,x}+\rho^{-1}p_{,x}=0\\ \left[\rho S\left(\varepsilon+\tfrac{1}{2}u_x^2\right)\right]_{,t}+\left[\rho S u_x\left(\varepsilon+\tfrac{1}{2}u_x^2\right)\right]_{,x}+\left(u_x S p\right)_{,x}=S f_e\\ \varepsilon=\frac{p}{k_1-1}\left(\frac{1}{\rho}-\frac{1-\psi}{\delta}-\alpha\psi\right),\quad f_e=\rho\frac{d\psi}{dt}\frac{f}{k_1-1},\quad \frac{d\psi}{dt}=\Gamma\left(\psi\right)f_s\left(p\right)\end{gathered} \tag{1}$$

$$\begin{gathered}\rho\left(x,0\right)=\omega,\ u_x\left(x,0\right)=0,\ p\left(x,0\right)=p_f,\\ \psi\left(x,0\right)=\frac{\left(p_f-p_z\right)\left(V_0-\dfrac{\omega}{\delta}\right)}{\omega\left[f+\left(p_f-p_z\right)\left(\alpha-\delta^{-1}\right)\right]}\end{gathered} \tag{2}$$

$$\begin{gathered}u_x\left(-l_B,t\right)=0,\quad u_x\left(x_L(t),t\right)=u_p(t)\\ \frac{du_p}{dt}=\frac{S_p\left[p\left(x_L(t),t\right)-p\left(x_P(t),t\right)\right]}{\varphi m_p},\ u_p\left(0\right)=0\\ \frac{dx_L}{dt}=u_p(t),\ x_L(0)=x_{L0}\end{gathered} \tag{3}$$

$$p\left(x_P(t),t\right)=p_{02}\left[\frac{U}{k_2+1}\left(U+\sqrt{U^2+4}\right)+1\right],\quad U=\frac{(k_2+1)u_p(t)}{2c_{02}} \tag{4}$$

Equations (1) are equations of balance of mass, momentum and energy for the 1D flow of gas in a duct with slowly changing cross section $S(x)$. The equations are supplemented by: the caloric equation of state for the polytropic gas obeying the Nobel-Abel equation of state, an expression for the volume intensity of heat sources f_e (burning of propellant) and the equation for the production of propellant gases due to burning of solid propellant. Functions $\Gamma(\psi)$ and $f_s(p)$ describe the dependence of the volumetric burning rate of the propellant on the relative volume of the burnt propellant and pressure. In the modelling, we assumed $f_s(p) = p$ and $\Gamma(\psi)$ corresponding to the geometrical law of propellant burning.

The initial conditions (2) determine the values of the flow parameters and the relative volume of the burnt propellant at the moment when pressure in the burning chamber attains the value of the starting pressure p_f. The boundary conditions (3) include the zero velocity condition at the base of the burning chamber, condition at the tail of the moving projectile, as well as the equation of motion and the equation of trajectory of the projectile. Equation (4) provides an estimate of the pressure acting on the projectile from the side of the air in the barrel. This estimate makes use of the relation between velocity and pressure at the front of a normal shock wave in the air.

The initial-boundary problem (1)-(3) was solved numerically by the method of characteristics [15].

2.2 Step 2 – precursor flow

In the second step, we used the commercial ANSYS FLUENT code for modelling the 2D axi-symmetric motion of air in the barrel and outside the muzzle. The function $u_p(t)$ was used as a boundary condition at the projectile surface. As a result of the modelling, we obtained a flow field in the air near the muzzle at the moment the outflow of propellant gases begins.

We consider the flow of air in the area shown in Figure 2 (in 3D and in 2D projection).

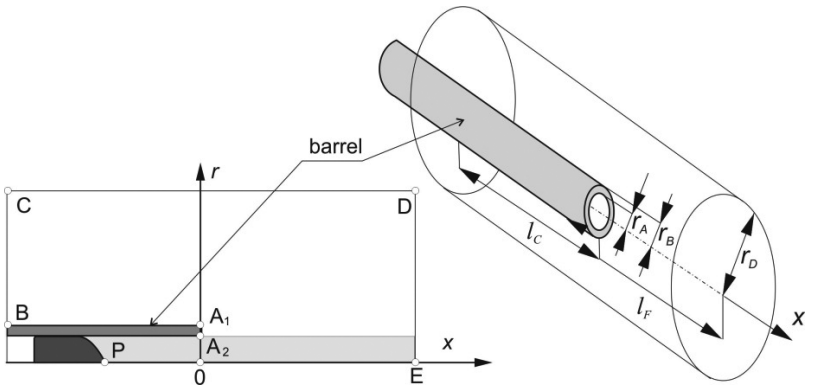

Figure 2. Area of the flow of air considered in the second step.

The mathematical model for the second step is given by the following initial-boundary problem:

$$
\begin{aligned}
&\rho_{,t}+\left(\rho u_x\right)_{,x}+r^{-1}\left(r\rho u_r\right)_{,r}=0\\
&\left(\rho u_x\right)_{,t}+\left(\rho u_x^2\right)_{,x}+r^{-1}\left(r\rho u_x u_r\right)_{,r}+p_{,x}=0\\
&\left(\rho u_r\right)_{,t}+\left(\rho u_x u_r\right)_{,x}+r^{-1}\left(r\rho u_r^2\right)_{,r}+r^{-1}\left(rp\right)_{,r}=0\\
&\left(\rho e\right)_{,t}+\left(\rho e u_x\right)_{,x}+r^{-1}\left(r\rho e u_r\right)_{,r}+\left(p u_x\right)+r^{-1}\left(rpu_r\right)_{,r}=0\\
&e=\varepsilon+\tfrac{1}{2}\left(u_x^2+u_r^2\right),\quad \varepsilon=\frac{p}{\rho(k_2-1)}
\end{aligned}
\tag{5}
$$

$$
\left\{\rho,u_x,u_r,p\right\}(x,r,0)=\left\{\rho_{02},0,0,p_{02}\right\}
$$

$$
x,r\in\left\{\begin{array}{c}
x\in\left[-l_C,l_F\right]\wedge r\in\left[r_B,r_D\right]\\
x\in\left[0,l_F\right]\wedge r\in\left[r_A,r_B\right]\\
x\in\left[x_p(0),l_F\right]\wedge r\in\left[0,r_A\right]\\
x\in\left[x_P(0)-l_{FP},x_P(0)\right]\wedge r=f_{SP}(x-x_P(0))
\end{array}\right\}
\tag{6}
$$

$$
\mathbf{F}\cdot n\left(x,r,t\right)\Big|_{boundary}=\mathbf{F}\cdot\vec{n}\left(x,r,t\right)\Big|_{inside}
$$

$$
x,r\in\left\{\begin{array}{c}
x=-l_C\wedge r\in\left[r_B,r_D\right]\\
x\in\left[-l_C,l_F\right]\wedge r=r_D\\
x=l_F\wedge r\in\left[0,r_D\right]
\end{array}\right\}\quad
\mathbf{F}=\begin{bmatrix}
\rho u_x & \rho u_r\\
\rho u_x^2+p & \rho u_x u_r\\
\rho u_r u_x & \rho u_r^2+p\\
\rho u_x^2+pu_x & \rho u_x^2+pu_r
\end{bmatrix}\quad
\vec{n}=\begin{bmatrix}n_x\\ n_r\end{bmatrix}
\tag{7}
$$

$$
\begin{aligned}
&\left(\vec{u}\cdot\vec{n}\right)(x,r,t)=0\\
&\left\{x,r\right\}\in\left\{\left\{x\in\left[-l_C,0\right],r=r_B\right\}\wedge\left\{x\in\left[x_P(t)-l_{FP},0\right],r=r_A\right\}\wedge\right.\\
&\left.\wedge\left\{x\in\left[0,l_F\right],r=0\right\}\wedge\left\{x=0,r=\in\left[r_A,r_B\right]\right\}\right\}
\end{aligned}
\tag{8}
$$

$$
\begin{aligned}
&\left(\vec{u}\cdot\vec{n}-u_P(t)\right)(x,r,t)=0,\\
&\left\{x,r\right\}\in\left\{x\in\left[x_P(t)-l_{FP},x_P(t)\right],r\in[0,f_{SP}\left(x-x_P(t)+x_P(0)\right)]\right\}
\end{aligned}
\tag{9}
$$

$$
\frac{dx_P}{dt}=u_P(t)
\tag{10}
$$

The boundary condition (7) is a non-reflecting boundary condition, having the form of an equality of fluxes at the outer boundaries BC, CD, DE (Figure 2) and in their vicinity inside the area in which the flow is modelled. The symbols n_x, n_r mean components of a unit vector normal to a boundary. The boundary condition (8) follows from the assumption that the normal component of the velocity vector at the outer and inner walls of the gun is equal to zero. The same condition is set at the axis of symmetry. The boundary condition (9) is set at the surface of the forward part of the projectile. Function $u_P(t)$ is a known function, determined in step 1.

The initial-boundary problem (5)-(9) was solved using the ANSYS FLUENT code. The area of flow was covered by a grid having approximately 20000 nodes and 20000 elements. The grid was made denser close to the muzzle, because this is an area of very rapid change in flow parameters. Quadrilateral elements were used except close to the region adjacent to the forward part of the projectile, where triangular elements were used to better fit the shape of the projectile. A density-based implicit solver was used. A moving grid was applied in the region shaded in Figure 2. Nodes and elements move with a velocity equal to the velocity of the projectile. The "Layering" option was used. Cells were disintegrated at the boundary DE.

2.3 Step 3 – propellant gases outflow

In the third step, we used ANSYS FLUENT for modelling the 2D axi-symmetric motion of air and propellant gases in the barrel and outside the muzzle. The spatial distributions of propellant gases flow parameters in the barrel and in the air outside the muzzle obtained in the first and the second steps were used as initial conditions.

We consider the flow of the air and propellant gases in the area, the 2D projection of which is shown in Figure 3.

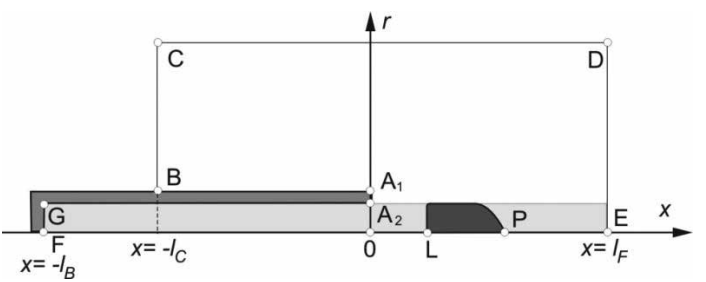

Figure 3. 2D projection of the area of flow considered in the third step.

The mathematical model for the third step is given by the set of Equations (5), boundary condition (7) and the following conditions:

$$\{\rho, u_x, u_r, p\}(x,r,0) = \{f_\rho(x,r), f_{ux}(x,r), f_{ur}(x,r), f_p(x,r)\}$$
$$x,r \in \begin{Bmatrix} x \in [-l_C, l_F] \wedge r \in [r_B, r_D] \\ x \in [0, l_F] \wedge r \in [r_A, r_B] \\ x \in [f_{SP}(r), l_F] \wedge r \in [0, r_A] \end{Bmatrix} \tag{11}$$

$$(\vec{u} \cdot \vec{n})(x,r,t) = 0 \quad \{x,r\} \in \{\{x \in [-l_C, 0], r = r_B\} \wedge \{x \in [-l_C, 0], r = r_A\} \wedge$$
$$\wedge \{x \in [-l_C, x_L(t)] \wedge [x_P(t), l_F], r = 0\} \wedge \{x = -l_B, r \in [0, r_A]\}\} \tag{12}$$

$$(\vec{u} \cdot \vec{n} - u_P(t))(x,r,t) = 0,$$
$$\{x,r\} \in \{x \in [x_P(t) - l_P, x_p(t)], r \in [0, f_{SP}(x - x_p(t) + x_p(0))]\} \tag{13}$$

$$\frac{dx_p}{dt} = u_p(t), \quad \frac{du_p}{dt} = \frac{2\pi}{m_p} \int_{-l_P}^{0} \int_{0}^{f_{SP}(\xi)} p(\xi + x_P(t) - l_P, t)\, n_x(\xi, \mu)\, \mu\, d\mu\, d\xi,$$
$$x_p(0) = l_p, u_p(0) = u_p(t_{k2}) \tag{14}$$

It was assumed that in the third step the propellant gases can be treated as a perfect gas. This assumption is justified by the fact that the initial pressure value is much lower than the maximum propellant gases pressure and it rapidly drops during the outflow of the gases. Functions $\rho(x,r)$, $u_x(x,r)$, $u_r(x,r)$, $p(x,r)$ determine the distributions of flow parameters at the moment of the beginning of the outflow of propellant gases. The boundary condition, Equations (13), is set at the moving surface of the projectile. The velocity of the projectile $u_p(t)$ was calculated by integrating the pressure distribution at the surface of the projectile, Equations (14). Its initial value was set to the value of the velocity of the projectile at the end of step two (t_{k2} is the final moment of step two).

As in step 2, the ANSYS FLUENT code was used. A moving grid was applied in the area shaded in Figure 3. Cells were disintegrated at the boundary DE and new cells were created at the line FG.

3 Results and Discussion

The results of calculations performed for a 30 mm launching system are presented. The calculations were performed for the following data: $\alpha = 1.174$ dm^3·kg^{-1}, $\delta = 1600$ kg·m^{-3}, $\Gamma(\psi) = 1.98\ 10^{-6}\ (1 - 0{,}4\psi)^{1/2}$ s^{-1}·Pa^{-1}, $\varphi = 1.02$, $\omega = 855$ kg·m^{-3}, $f = 0.9894$ MJ·kg^{-1}, $k_1 = 1.2$, $l_B = 2.69$ m, $m_p = 0.3658$ kg, $p_f = 40$ MPa, $p_z = 4$ MPa, $x_{L0} = -2.56$ m.

The calculated velocity history determined for step 1 is presented in Figure 4 (zero time corresponds to the moment when the projectile starts to move). The pressure and velocity distributions at the final moment of the motion of the projectile are presented in Figure 5 (crosshairs). They are very close to the constant pressure and linear velocity distributions assumed in the classical models of internal ballistics [2] (solid lines). This confirms that using a 1D model in the first step is a rational choice.

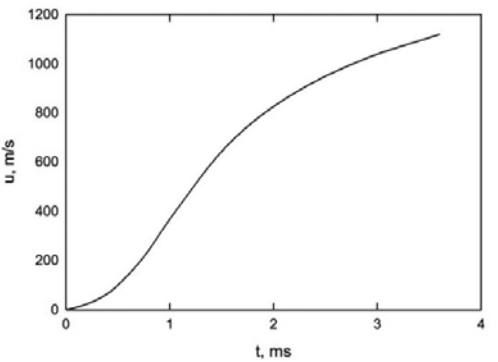

Figure 4. History of the projectile velocity determined for step 1.

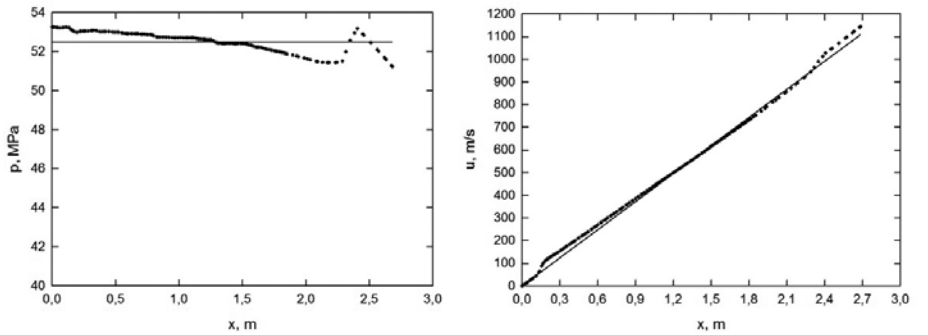

Figure 5. Pressure and velocity distributions in the propellant gases determined for step 1 (solid lines – results of calculations using a classical internal ballistics model [2]).

The results of calculations for the third step are presented in Figure 6, showing changes over time of the mean pressure acting on the tail end of the projectile (zero time corresponds to the moment when the projectile leaves the muzzle). The pressure acting on the tail drops very quickly and after approx. 0.15 ms approaches the value of the pressure acting on the forward part. This is the moment defining the end of the acceleration of the projectile. From this moment the velocity remains practically constant up to the end of the intermediate ballistics period (Figure 7).

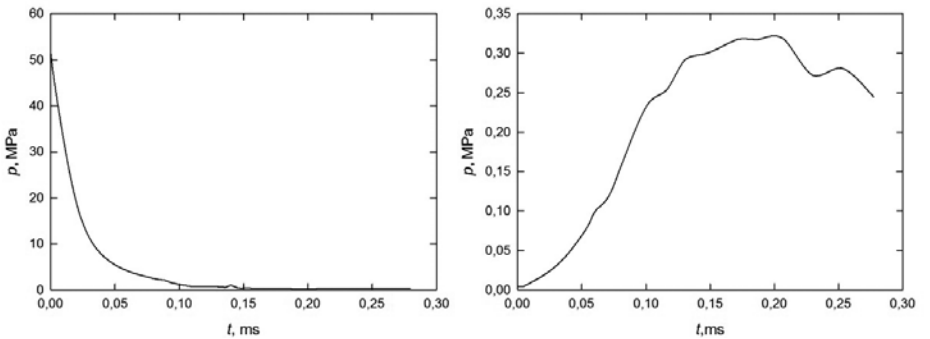

Figure 6. Mean pressure changes over time acting on the rear and forward part of the projectile, respectively.

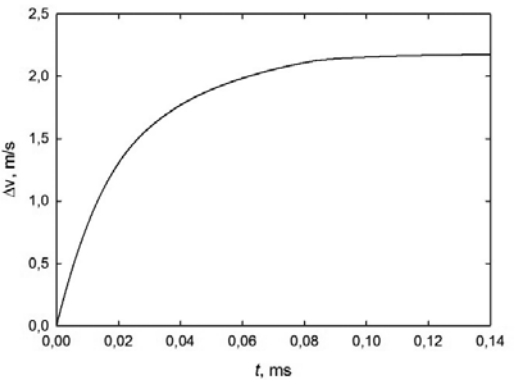

Figure 7. History of the increase in projectile velocity determined for step 3.

The relative velocity increase in the intermediate ballistics period is approx. 0.2% and it is almost one order of magnitude lower than expected. Analyzing the available experimental data, we came to the conclusion that such a small effect could not be detected by the Doppler velocimetry used in [6], because the

results of the measurements were perturbed by oscillations much larger than the calculated velocity increase.

Looking for experimental data that could confirm the correctness of the results of our modelling, we invoked the results of measurements of acceleration of projectiles presented in [16] and [17]. Although the measurements of acceleration are highly perturbed for the intermediate period, approximating the results of the measurements by an exponential decay gives information about changes of the pressure acting on the projectile over time. Due to the lack of data concerning the 155 mm launching system used in [16], we performed calculations for another 155 mm launching system. Figure 8 shows a comparison of the calculated pressure *vs.* time changes and an approximation taken from [16]:

$$p(t) = p_m e^{-\beta t}, \quad p_0 = 68.9 \text{ MPa}, \quad \beta = 5777 \text{ s}^{-1} \tag{15}$$

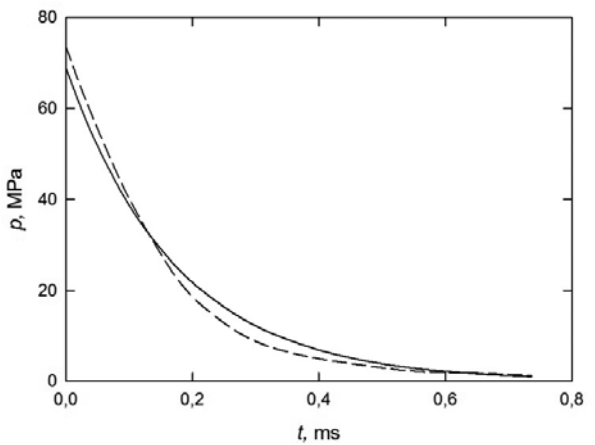

Figure 8. Pressure *vs*. time in the intermediate period for 155 caliber launching systems: solid line – approximation (15) [16], dashed line – results of modeling.

Despite the fact that the $p(t)$ curves refer to different 155 mm launching systems, they are very close. Taking into account that the velocity increase Δu is proportional to the area under both curves, we can conclude that our model properly estimates the magnitude of Δu.

Values of the velocity increase were calculated for ten launching systems, from small to large calibers. The results of these calculations are presented in Table 1. The largest values of the relative velocity increase were obtained for launching systems with a low muzzle velocity (9 mm and 122 mm). In these

cases the flow behind the projectile at the end of the internal ballistics period is subsonic. This means that a rarefaction wave enters the barrel at the initial moment and this additionally accelerates the propellant gases. This acceleration has the effect that the velocity of the propellant gases at the muzzle can be much larger than the velocity of the projectile. This causes a more prolonged action of the propellant gases flow on the projectile. Because of this, the relative velocity increase is larger.

Table 1. Results of calculations of the velocity increase in the intermediate ballistics period

Caliber, [mm]	Δu_{CFD}, [m·s^{-1}]	$\Delta u_{CFD}/u_m$, [%]
5.56 (1)*	2.68	0.3
5.56 (2)**	3.40	0.4
7.62	2.70	0.3
9	5.11	1.4
12.7	2.50	0.5
14.5	5.96	0.5
23	3.80	0.4
30	2.38	0.2
122	2.03	0.8
155	5.01	0.5

*Assault rifle Beryl; ** New assault rifle under development.

4 Conclusions

The main results of the work can be summarized as follows:

1. The increase in the projectile velocity in the intermediate ballistics period is relatively small – parts per thousand of the muzzle velocity. Only for a very low muzzle velocity can it be larger than 1%.
2. Differences between the results of the internal ballistics calculations and the initial velocity used in the external ballistics models cannot be attributed to the phenomena taking place in the intermediate ballistics period. The muzzle velocity calculated by the use of the internal ballistics models can be accepted as the initial velocity for the external ballistics models. The accuracy of this value depends on the precision of the internal ballistics models.
3. The maximum velocity is attained at a distance of several calibers. Therefore, it is acceptable to assume, in the external ballistics models, that the maximum velocity is attained at the position of the muzzle.

5 References

[1] Klingenberg G., Heimerl J.M., *Gun Muzzle Blast and Flash* (Progress in Astronautics and Aeronautics, Vol. 139), AIAA, **1988**.

[2] Serebryakov M.E., *Internal Ballistics of Gun Systems and Solid Propellant Rockets* (in Russian), Oborongiz, Moscow, **1962**.

[3] Carlucci D.E., Jacobson S.S., *Ballistics: Theory and Design of Guns and Ammunition*, CRC Press, Boca Raton – London – New York, **2008**.

[4] *Gun Propulsion Technology*, Vol. 109, Progress in Astronautics and Aeronautics (M. Summerfield & L. Stiefel, Eds.), **1988**.

[5] Leciejewski Z., Surma Z., Torecki S., Trebinski R., Czyzewska M., Baranowski L., *Theoretical-experimental Investigations on Propellant Gases Outflow Influence on the Parameters of the Motion of Projectiles* (in Polish), Report on Project 533/B/T00/2009/37 financed by the Ministry of Science and Higher Education in the period 2009-2012.

[6] Szapiro J., *External Ballistics* (in Polish), MON, Warszawa, **1956**.

[7] Leciejewski Z., Surma Z., Torecki S., Trebinski R., Czyzewska M., Theoretical and Experimental Investigations of Projectile Motion Specificity in the Intermediate Period, *Proc. Int. Symp. Ballist., 27th*, Freiburg, Germany, **2013**, 333-343.

[8] Erdos J.I., Del Guidice P.D., Calculation of Muzzle Blast Flowfields, *AIAA Journal*, **1975**, *13*(8), 1048-1055.

[9] Moretti G., A Numerical Analysis of Muzzle Blast Precursor Flow, *Comput. Fluids*, **1982**, *10*(1), 51-86.

[10] Cayzac R., Carette E., Alziary de Roquefort T., Vaglio C., Brossard J., Intermediate Ballistic Computations and Validation, *Proc. Int. Symp. Ballist., 17th*, Midrand, South Africa, **1998**, *2*, 1-8.

[11] Jiang Z., Takayama K., Skews B.W., Wave Interactions Following the Emergence of a Supersonic Projectile from a Tube, *Proc. Int. Symp. Ballist., 17th*, Midrand, South Africa, **1998**, *2*, 9-16.

[12] Hudson M.K., Luchini C., Clutter J.K., Shyy W., The Evaluation of Computational Fluid Dynamics Methods for Design of Muzzle Blast Suppressors for Firearms, *Propellants Explos. Pyrotech.*, **2001**, *26*(4), 201-208.

[13] Bin J., Kim M., Lee S., A Numerical Study on the Generation of Impulsive Noise by Complex Flows Discharging from a Muzzle, *International Journal for Numerical Methods in Engineering*, **2008**, *75*(8), 964-991.

[14] Jiang X., Chen Z., Fan B., Li H., Numerical Simulation of Blast Flow Fields Induced by a High-speed Projectile, *Shock Waves*, **2008**, *18*(3), 205-212.

[15] Betekhtin S.A., Vinitskii A.M., Gorokhov N.A., *Gasdynamic Fundamentals of Internal Ballistics* (in Russian), Oborongiz, Moscow, **1957**.

[16] Carlucci D., Vega J., Empirical Relationship for Muzzle Exit Pressure in a 155 mm Gun Tube, *WIT Trans. Modell. Simul.*, **2007**, *45*, 225-229.

[17] Carlucci D., Frydman A.M., Cordes J.A., Mathematical Description of Projectile Shot Exit Dynamics (Set-Forward), *J. Appl. Mech.*, **2013**, *80*, 031501-1-9.